Statistical and Dynamical Properties
of the Discrete Sinai Model
at Finite Times

J. Chave,

CEA, Service de Physique de l'Etat Condensé,

F-91191 Gif sur Yvette Cedex, France

E. Guitter

CEA, Service de Physique Théorique de Saclay,

F-91191 Gif sur Yvette Cedex, France

We study the Sinai model for the diffusion of a particle in a one dimensional quenched random energy landscape. We consider the particular case of discrete energy landscapes made of random ± 1 jumps on the semi infinite line $\mathbb{Z}^+$ with a reflecting wall at the origin. We compare the statistical distribution of the successive local minima of the energy landscapes, which we derive explicitly, with the dynamical distribution of the position of the diffusing particle, which we obtain numerically. At high temperature, the two distributions match only in the large time asymptotic regime. At low temperature however, we find even at finite times a clear correspondence between the statistical and dynamical distributions, with additional interesting oscillatory behaviors.

email: chave@spec.saclay.cea.fr, guitter@spht.saclay.cea.fr

1. Introduction

The problem of the diffusion of a particle in a one dimensional quenched random energy landscape has been studied for many years [1,2]. If the landscape itself has a random walk statistics, many exact predictions exist for the *long time behavior* of the diffusion process. For an unbiased statistics of the potential, i.e in the absence of drift, the average distance $\langle x \rangle$ traveled by the particle grows very slowly at large times, with the Sinai scaling behavior $\langle x \rangle \sim (T \ln(t))^2$, where T is the temperature [2]. The asymptotic probability distribution is universal in the scaling variable $x/(T \ln(t))^2$ and its precise form is known exactly for a single diffusing particle [3-5]. Moreover, the thermal dispersion (or the distance between two diffusing particles in the same random potential) remains finite at large times [6]. The physical picture underlying these results is simply that of a *localization* of the diffusing particle in the deepest energy minimum which it can reach at time t by passing larger and larger energy barriers [6-7].

These large time asymptotic predictions were tested numerically by computing the *exact* probability distribution for the position x of the particle at finite but large enough times t for energy landscapes drawn at random, and then averaging over a large enough sample of such landscapes [8-10]. One should notice that the Sinai scaling $\langle x \rangle \sim (T \ln(t))^2$ defines a very slow diffusive process. For such a process, the long time behavior is expected to be reached in practice after extremely long transients, especially at low temperature. Such times can be out of reach in practical situations or in finite time numerical simulations. This probably explains why the asymptotic predictions are not fully recovered in [8]. In any case, very little is known about the finite time behavior of the model or about the approach to the asymptotic regime.

In practice, the localization of the particle in the deepest minimum has the nice consequence that some of the *dynamical* properties of the diffusion process can be deduced directly from the corresponding *statistical* properties of the minima of the random potential. More precisely, the underlying idea is to assume that, at times of order t, the particle is localized in the deepest minimum of the energy landscape which it could reach by passing all the energy barriers ΔE of height less or equal to $\Gamma \sim T \ln(t)$. The time dependence of various quantities in the dynamical process can then be obtained from the equilibrium *statistics* of the energy minima and its dependence in the highest passable energy barrier Γ. This idea has been implemented recently to develop a new Real Space Renormalization Group (RSRG) approach for the Sinai model [11]. The RSRG formalism consists in performing a suitable decimation of the barriers with height less than Γ to obtain universal Renormalization Group equations for the variation with increasing Γ of the effective energy landscape distribution seen by the particle at the time scale t. Long time properties are obtained from the $\Gamma \to \infty$ fixed point of these RSRG equations. This technique allows to recover the universal asymptotic probability distribution of a single particle for various boundary conditions. It also allows for the prediction of asymptotic two-time or two-particle correlations.

Following the above "statistical picture" leading to the exact asymptotic predictions, one may wonder whether this picture could also help to investigate shorter times or very low temperatures. In this paper, we test the connection between the dynamical properties of the diffusion process and the statistics of the minima of the energy landscapes for finite

times. We use a particular distribution of the disorder where the energy landscapes are made of successive random ± 1 increments, i.e. have the statistics of a *discrete* random walk. The reason for this choice is twofold. On the one hand, we can easily derive *explicit* laws for the statistics of minima at arbitrary (even small) Γ. On the other hand, this is particularly adapted to numerical simulations of the dynamical process. As we shall see, our results corroborate the statistical picture, not only at large Γ where we recover the universal distributions expected for general random energy landscapes with a random walk statistics, but also at small Γ *and* low temperature, where the discrete nature of the energy landscapes is sensible and yields interesting behaviors.

The paper is organized as follows. In Section 2, we briefly describe the particle diffusion process and the distribution for the random energy landscapes. In Section 3, we derive explicit formulas for the statistics of energy minima in the presence of energy barriers of arbitrary scale Γ. Section 4 presents numerical results for the dynamical diffusion process. These results are compared with the predictions of the statistical approach of Section 3. We gather our conclusions in Section 5.

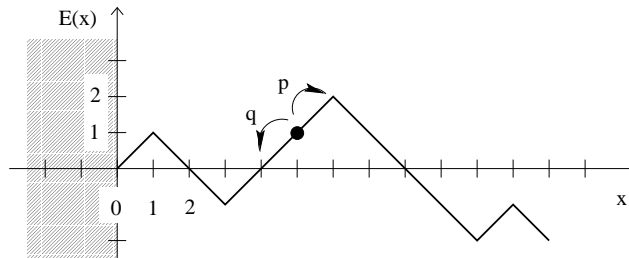## 2. Diffusion of a particle in a discrete random energy landscape

Fig.1: A discrete random energy landscape $E(x)$. A reflecting wall prevents the particle from exploring the negative x region. The particle jumps to the left or to the right with the probabilities given by equation (2.2).

We consider the following discrete distribution for the quenched energy landscapes. On each site $x = 0, 1, 2, ...$ labeled by a non negative integer, we associate a random energy variable $E(x)$ such that (see Figure 1)

$$E(0) = 0$$
$$\Delta E(x) = E(x+1) - E(x) = \pm 1 \tag{2.1}$$

The sign ± 1 of the increment is drawn at random between successive sites with even probability $1/2$, i.e. we introduce no drift in the problem. With the choice (2.1), the values of the energy are limited to integers, meaning that we have implicitly fixed an underlying energy scale. We can view $E(x)$ as the "height" at site x of a discrete random walk describing our energy landscape. We finally set $E(-1) = +\infty$, i.e. put an infinite reflecting wall on the negative side of the origin, while we keep a free boundary condition

2

at $x = +\infty$. This choice of boundary condition is clearly not crucial but makes our analysis simpler since in this case, deeper minima always appear at increasing values of x.

For a given realization of the quenched random energy landscape, we consider the following discrete time dynamical process:

- We start at time $t = 0$ at position $x = 0$ with energy $E(0) = 0$.
- Given the position x with energy $E(x)$ at time t, the position at time $t + 1$ is

$$\begin{cases} x + 1 \text{ with probability } p_x \equiv \dfrac{e^{-\beta \Delta E(x)}}{e^{-\beta \Delta E(x)} + e^{\beta \Delta E(x-1)}} \\[4mm] x - 1 \text{ with probability } q_x \equiv \dfrac{e^{\beta \Delta E(x-1)}}{e^{-\beta \Delta E(x)} + e^{\beta \Delta E(x-1)}} \end{cases} \tag{2.2}$$

with $\Delta E(x)$ as in (2.1) and $\beta = 1/T$ the inverse temperature.

With the choice (2.1) for the variation of the energy on neighboring sites, the ratio p_x/q_x is equal to 1 if the two sites $x+1$ and $x-1$ have the same energy, or to $\exp(\pm 2/T)$ if they have different energies. Note that the case $x = 0$ is special with $p_0 = 1 - q_0 = 1$. Note also that the particle has to move to one of its neighboring sites at each time step, i.e. we do not allow the particle to remain at the same site. As a consequence, the particle occupies sites with even position at even times and sites with odd position at odd times. This effect results in "residual fluctuations" even at $T = 0$. The above model is very simple since it depends on only one parameter, the temperature T. We study its behavior numerically in Section 4 but let us first derive explicit laws for the minima of energy landscapes with the discrete random walk statistics (2.1).

3. Statistics of energy minima

In this section, we forget for a while the dynamical process and focus on the statistics of the successive minima of the random energy landscapes which can be reached in the presence of increasingly passable energy barriers. Following [11], we consider for any given realization of the energy landscape the position $x = x_{\min}(\Gamma)$ of the *deepest* minimum of this landscape which can be reached, starting from the wall at the origin $x = 0$, by passing through energy barriers of height *less or equal* to a fixed scale Γ. Here $x_{\min}$ and Γ are non negative integers. For each Γ, we compute the probability $p_\Gamma(x)$ that $x_{\min}(\Gamma)$ equals x, obtained by averaging the quantity $\delta_{x,x_{\min}(\Gamma)}$ over all realizations of the energy landscape. Note that, for a given realization, the deepest reachable minimum is not necessarily unique but can be degenerate. We will thus consider three different probabilities $p_\Gamma^{(1)}(x)$, $p_\Gamma^{(2)}(x)$ and $p_\Gamma^{(3)}(x)$, corresponding respectively to the following prescriptions in case of degeneracy:
(1) we keep only the closest minimum to the origin,
(2) we keep only the furthest minimum from the origin,
(3) we take the average over all the degenerate minima, i.e. consider the quantity $(1/k)\sum_{i=1}^{k} \delta_{x,x_{\min}^{(k)}}$ for k degenerate minima at position $x_{\min}^{(k)}$.
We shall give below explicit formulas for the generating functions

$$\mathcal{P}_\Gamma^{(i)}(z) = \sum_{x=0}^{\infty} p_\Gamma^{(i)}(x) z^x \quad i = 1, 2, 3 \tag{3.1}$$

3.1. Random walk in a strip of height Γ

Before we proceed, we need to evaluate the probability $d_\Gamma(x)$ for a random walk starting at $E(0) = 0$ to have its x first steps inside the strip $0 \leq E \leq \Gamma$ and its $(x+1)$th step at $E(x+1) = -1$, i.e. the probability for the walk to leave the strip for the first time just after position x and downwards. We recall here the explicit form of the generating function $D_\Gamma(z) = \sum_x d_\Gamma(x) z^x$. In the following, we will always assume that the $(x+1)$th step points downwards, which in practice occurs with probability $1/2$, i.e. we will calculate $2D_\Gamma(z)$ instead of $D_\Gamma(z)$.
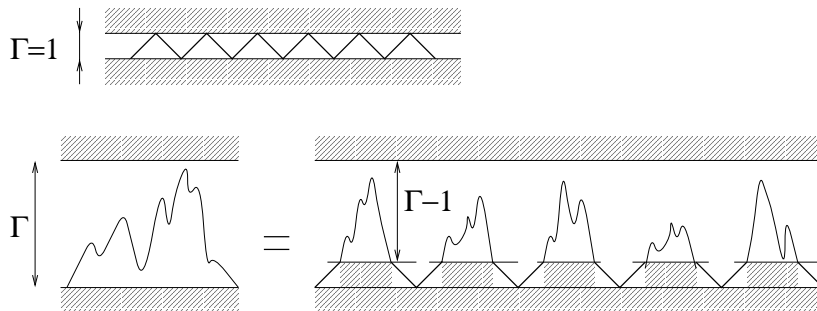

Fig.2: For a strip of height $\Gamma = 1$, the random walk is a series of $E = 0 \to 1 \to 0$ two-step-sequences. To obtain $2D_\Gamma(z)$, each two-step-sequence must be dressed with a factor $2D_{\Gamma-1}(z)$ in the middle.

The function $D_\Gamma(z)$ satisfies the recursion relation:

$$D_\Gamma(z) = \frac{1}{2 - z^2 D_{\Gamma-1}(z)} \tag{3.2}$$

with the initial condition $2D_0(z) = 1$ (for $\Gamma = 0$, the first exit from the zero-width strip occurs necessarily just after $x = 0$). This relation can be understood as follows (see Figure 2): consider the case $\Gamma = 1$, for which the random walk is necessarily of even length x and made of the repetition of $x/2$ elementary two-step-sequences of the type $(E = 0 \to 1 \to 0)$. Each two-step-sequence comes with a factor z^2 in the generating function and occurs with a probability $(1/2)^2$, leading to,

$$2D_1(z) = \sum_{\substack{x=0 \\ x \,\mathrm{even}}}^{\infty} \left(\frac{z^2}{2^2}\right)^{\frac{x}{2}} = \frac{1}{1 - \left(\frac{z}{2}\right)^2} \tag{3.3}$$

in agreement with (3.2) and $D_0(z) = 1/2$. The generating function $2D_\Gamma(z)$ can be obtained in the same way by replacing the weight $(z/2)^2$ for the elementary two-step-sequence by a weight $(z/2)^2 \times 2D_{\Gamma-1}(z)$, corresponding to inserting between the two steps $E = 0 \to 1$ and $E = 1 \to 0$ an arbitrary sequence of steps limited to the strip of width $\Gamma - 1$, $1 \leq E \leq \Gamma$ (see Figure 2). Making this replacement in (3.3) directly leads to (3.2).

From (3.2), we can write the generating function $D_\Gamma(z)$ as the ratio:

$$D_\Gamma(z) = \frac{P_\Gamma(z)}{P_{\Gamma+1}(z)} \tag{3.4}$$

4

where $P_\Gamma(z)$ is an even polynomial of degree $2[\Gamma/2]$ in the variable z. Indeed, writing $D_\Gamma(z) = P_\Gamma(z)/Q_\Gamma(z)$, (3.2) gives

$$\frac{P_\Gamma(z)}{Q_\Gamma(z)} = \frac{1}{2 - z^2 \frac{P_{\Gamma-1}(z)}{Q_{\Gamma-1}(z)}} = \frac{Q_{\Gamma-1}(z)}{2Q_{\Gamma-1}(z) - z^2 P_{\Gamma-1}(z)} \tag{3.5}$$

leading to recursion relations

$$P_\Gamma(z) = Q_{\Gamma-1}(z)$$
$$Q_\Gamma(z) = 2Q_{\Gamma-1}(z) - z^2 P_{\Gamma-1}(z) \tag{3.6}$$

Eliminating Q_Γ, we get the announced result (3.4), with, moreover, the recursion relation

$$P_{\Gamma+1}(z) - 2P_\Gamma(z) + z^2 P_{\Gamma-1}(z) = 0 \tag{3.7}$$

which determines $P_\Gamma(z)$ from the initial values $P_0(z) = 1$ and $P_1(z) = 2$. Setting

$$P_\Gamma(z) = z^\Gamma U_\Gamma \left(\frac{2}{z} \right) \leftrightarrow U_\Gamma(y) = \left(\frac{y}{2} \right)^\Gamma P_\Gamma \left(\frac{2}{y} \right) \tag{3.8}$$

the above recursion relation transforms into

$$U_{\Gamma+1}(y) - yU_\Gamma(y) + U_{\Gamma-1}(y) = 0 \tag{3.9}$$

with $U_0(y) = 1$ and $U_1(y) = y$. The solution of this recursion is given by the well known Chebishev polynomials $U_\Gamma(z)$, characterized by

$$U_\Gamma(2\cosh(t)) = \frac{\sinh((\Gamma+1)t)}{\sinh(t)} \tag{3.10}$$

We thus get the explicit form:

$$P_\Gamma \left(\frac{1}{\cosh(t)} \right) = \frac{1}{(\cosh(t))^\Gamma} \frac{\sinh((\Gamma+1)t)}{\sinh(t)} \tag{3.11}$$

and the explicit formula:

$$D_\Gamma \left(z = \frac{1}{\cosh(t)} \right) = \cosh(t) \frac{\sinh((\Gamma+1)t)}{\sinh((\Gamma+2)t)} \tag{3.12}$$

The relation between $D_\Gamma(z)$ and the Chebishev polynomials is also derived in [12] in the context of the Temperley-Lieb algebra. In the limit $t \to 0$, we get the particular result

$$D_\Gamma(1) = \frac{\Gamma+1}{\Gamma+2} \tag{3.13}$$

which is the probability for the walk to leave the strip $0 \le E \le \Gamma$ downwards at $E = 0$ rather that upwards at $E = \Gamma$. In the limit $\Gamma \to \infty$, we have

$$D_\Gamma(z) \overset{\Gamma \to \infty}{\to} \frac{1 - \sqrt{1 - z^2}}{z^2} \tag{3.14}$$

which, up to normalizations, is the generating function of Catalan numbers, counting closed walks on the semi-infinite line $E \ge 0$, as it should.

3.2. Explicit forms of $\mathcal{P}_\Gamma^{(i)}(z)$

We now come to the evaluation of the generating functions $\mathcal{P}_\Gamma^{(i)}(z)$ defined by (3.1). Given an arbitrary landscape of infinite length and for a given Γ, we have to look for the deepest minimum which can be reached by passing barriers of height less or equal to Γ. To do so, we decompose the random walk defining the landscape according to the following algorithm:

1/ Starting at $x_0 = 0$ and $E(x_0) = 0$, the walk has a first part entirely included in the strip of width Γ, $0 \le E \le \Gamma$. In this part, the last return at $E = 0$ occurs at some position x_1 (possibly 0). This defines a first building block of size x_1.

2/ Since x_1 is the last return at $E = 0$ within the strip of size Γ, two situations may occur for the remaining part of the walk:

    2-1/ Either the walk reaches $E = \Gamma + 1$ without returning to $E = 0$, i.e. the walk leaves the strip upwards. In this case, we have reached a barrier too high to be passed and we stop the process.

    2-2/ Or $E(x_1 + 1) = -1$, i.e. the walk leaves the strip downwards. In this case we repeat the process 1, i.e starting at position $x_1 + 1$ with $E(x_1 + 1) = -1$, we consider the following part of the walk entirely in the strip of height Γ, $-1 \le E \le \Gamma - 1$ and look for the position x_2 of the last return to $E = -1$ within this strip, defining a second block of size $x_2 - x_1 - 1$. We repeat the process until it is stopped by a too high barrier. The number $\mathcal{E}$ of building blocks is simply related to the height $1 - \mathcal{E}$ of the deepest minimum which could be reached. The position of this minimum can be obtained by properly summing the sizes of the blocks.

This algorithm is illustrated in Figure 3. To compute $\mathcal{P}_\Gamma^{(i)}(z)$, we simply have to assign a weight $2D_\Gamma(z)$ per building block and a factor $(z/2)$ for each descending bond between building blocks. The different prescriptions in case of degenerate minima concern only the last building block. In the case (1) of the closest minimum to the origin, the size of this block does not contribute to the position x_{min} of the minimum. This block thus comes with a factor 1. Summing over the number $\mathcal{E}$ of blocks, we deduce that $\mathcal{P}_\Gamma^{(1)}(z)$ is proportional to (see Figure 3-1):

$$\mathcal{P}_\Gamma^{(1)}(z) \propto 1 + 2D_\Gamma(z)\frac{z}{2} + \left(2D_\Gamma(z)\frac{z}{2}\right)^2 + \ldots = \frac{1}{1 - zD_\Gamma(z)} \qquad (3.15)$$

The normalization factor is fixed by demanding that $\mathcal{P}_\Gamma^{(1)}(1) = 1$ since, for $z = 1$, the generating function gives the probability to find the minimum at some arbitrary position x. We thus get:

$$\mathcal{P}_\Gamma^{(1)}(z) = \frac{1 - D_\Gamma(1)}{1 - zD_\Gamma(z)} \qquad (3.16)$$

Note that from the previous subsection, we can also understand the prefactor $1 - D_\Gamma(1)$ as the probability for the random walk to eventually leave the strip of size Γ upwards rather than going downwards. For the prescription (2), where we choose the furthest minimum from the origin, we have an extra factor $2D_\Gamma(z)$ for the last building block. We thus get
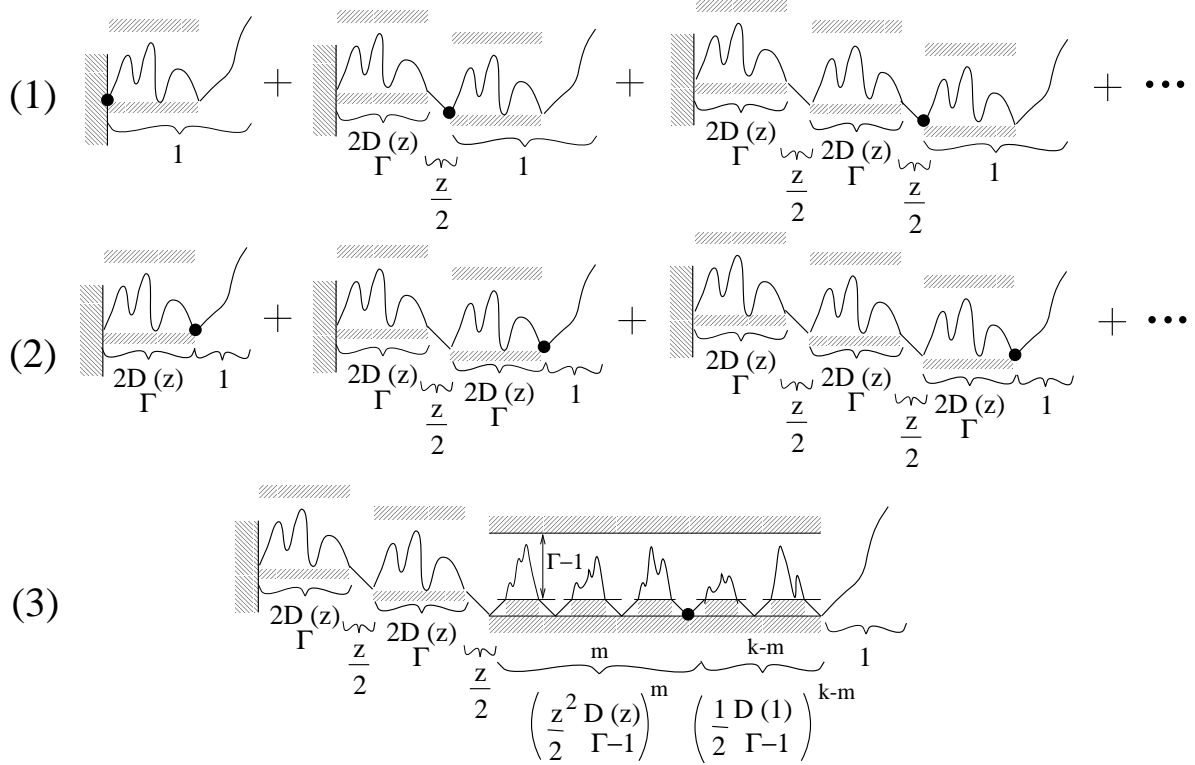
Fig.3: A schematic picture of the decomposition of random walks into building blocks. The number $\mathcal{E}$ of building blocks is related to the height $1 - \mathcal{E}$ of the deepest minimum reached without passing a barrier of size greater than Γ. For the different building blocks, we have also indicated the weights obtained by the average over the random walks to reconstruct the appropriate generating function $\mathcal{P}_\Gamma^{(i)}$. These weights depend on the precise prescription for degenerate minima: (1) keep the closest minimum to the origin; (2) keep the furthest minimum from the origin; (3) average over the minima.

in this case (see Figure 3-2):

$$\mathcal{P}_\Gamma^{(2)}(z) \propto 2D_\Gamma(z) + 2D_\Gamma(z)\frac{z}{2}2D_\Gamma(z) + \left(2D_\Gamma(z)\frac{z}{2}\right)^2 2D_\Gamma(z) + \ldots = \frac{2D_\Gamma(z)}{1 - zD_\Gamma(z)} \quad (3.17)$$

and:

$$\mathcal{P}_\Gamma^{(2)}(z) = \frac{D_\Gamma(z)}{D_\Gamma(1)} \times \frac{1 - D_\Gamma(1)}{1 - zD_\Gamma(z)} \quad (3.18)$$

The difference between the two cases (1) and (2) is thus simply a prefactor $D_\Gamma(z)/D_\Gamma(1)$ coming from the last building block. This factor is nothing but the generating function $\sum_x e_\Gamma(x)z^x$ associated with the probability $e_\Gamma(x)$ to find the furthest minimum at a distance x from the closest minimum.

The prescription (3), where we average over all minima in the case of degeneracy is more subtle. Here again, it concerns only the weight of last building block and leads to a different prefactor. Suppose we have $k + 1$ degenerate minima, each minimum will receive

a weight $1/(k+1)$. For the $(m+1)$'th minimum among the $k+1$, we have to assign a factor z only to the elementary steps of the walk which are to the left of the minimum while the steps which are to the right do not contribute to $x_{\text{min}}^{(m+1)}$ and receive a factor 1 instead. Still the right part of the block is important to guaranty that the total number of minima is precisely $k+1$. The generating function between successive minima is thus simply $2D_{\Gamma-1}(z)(z/2)^2$ on the left side of the chosen minimum and $2D_{\Gamma-1}(1)(1/2)^2$ on its right side (see Figure 3-3). The prefactor associated with the last block is now proportional to:

$$\sum_{k=0}^{\infty} \frac{1}{k+1}\left\{\sum_{m=0}^{k}\left(\frac{z^2 D_{\Gamma-1}(z)}{2}\right)^m\left(\frac{D_{\Gamma-1}(1)}{2}\right)^{k-m}\right\}$$

$$= \frac{1}{\frac{z^2 D_{\Gamma-1}(z)}{2} - \frac{D_{\Gamma-1}(1)}{2}}\ln\left(\frac{1 - \frac{z^2 D_{\Gamma-1}(z)}{2}}{1 - \frac{D_{\Gamma-1}(1)}{2}}\right) \tag{3.19}$$

$$= \frac{2D_\Gamma(z)D_\Gamma(1)}{D_\Gamma(z) - D_\Gamma(1)}\ln\left(\frac{D_\Gamma(z)}{D_\Gamma(1)}\right)$$

where we have used (3.2). We finally get

$$\mathcal{P}_\Gamma^{(3)}(z) = \frac{D_\Gamma(z)}{D_\Gamma(z) - D_\Gamma(1)}\ln\left(\frac{D_\Gamma(z)}{D_\Gamma(1)}\right) \times \frac{1 - D_\Gamma(1)}{1 - zD_\Gamma(z)} \tag{3.20}$$

by adjusting the normalization to guaranty that $\mathcal{P}_\Gamma^{(3)}(1) = 1$. Note that, as for (3.18), the prefactor involves only a function of $D_\Gamma(z)/D_\Gamma(1)$.

The formulas (3.16)-(3.20) can be made more explicit by use of (3.12), leading to

$$\mathcal{P}_\Gamma^{(1)}\left(z = \frac{1}{\cosh(t)}\right) = \frac{1}{\Gamma+2} \times \frac{\sinh\left((\Gamma+2)t\right)}{\sinh\left((\Gamma+2)t\right) - \sinh\left((\Gamma+1)t\right)}$$

$$\mathcal{P}_\Gamma^{(2)}\left(z = \frac{1}{\cosh(t)}\right) = \frac{1}{\Gamma+1} \times \frac{\cosh(t)\,\sinh\left((\Gamma+1)t\right)}{\sinh\left((\Gamma+2)t\right) - \sinh\left((\Gamma+1)t\right)}$$

$$\mathcal{P}_\Gamma^{(3)}\left(z = \frac{1}{\cosh(t)}\right) = \frac{\cosh(t)\,\sinh\left((\Gamma+1)t\right)}{\sinh\left((\Gamma+2)t\right) - \sinh\left((\Gamma+1)t\right)}\ln\left[\frac{\Gamma+2}{\Gamma+1}\frac{\cosh(t)\,\sinh\left((\Gamma+1)t\right)}{\sinh\left((\Gamma+2)t\right)}\right]$$

$$\times \frac{\sinh\left((\Gamma+2)t\right)}{(\Gamma+2)\cosh(t)\,\sinh\left((\Gamma+1)t\right) - (\Gamma+1)\sinh\left((\Gamma+2)t\right)} \tag{3.21}$$

These expressions constitute our central result describing the statistics of minima at finite Γ for the particular distribution of landscapes that we study.

At large Γ, an appropriate scaling limit can be obtained by a suitable scaling of z:

$$z = 1 - \frac{s}{\Gamma^2} \quad i.e. \quad t = \frac{\sqrt{2s}}{\Gamma} + \mathcal{O}\left(\frac{1}{\Gamma^3}\right) \tag{3.22}$$

This corresponds to setting

$$x = \Gamma^2 l \tag{3.23}$$

8

in the original probabilities $p_\Gamma^{(i)}(x)$. In this limit, the three generating functions $\mathcal{P}_\Gamma^{(i)}$ tend to the same limiting distribution $\mathcal{P}_\infty(s)$, equal to:

$$\mathcal{P}_\infty(s) = \frac{\tanh(\sqrt{2s})}{\sqrt{2s}} \tag{3.24}$$

This distribution is now the Laplace transform

$$\mathcal{P}_\infty(s) = \int_0^\infty dl\, p_\infty(l) e^{-sl} \tag{3.25}$$

of the limiting probability density

$$p_\infty(l) = \lim_{\Gamma \to \infty} \Gamma^2\, p^{(i)}(x = \Gamma^2 l) \quad i = 1, 2, 3 \tag{3.26}$$

From (3.24), we get

$$p_\infty(l) = \sum_{k=0}^\infty e^{-\frac{(2k+1)^2}{8}\pi^2 l} \tag{3.27}$$

The formulas (3.24) and (3.27) are actually more general and valid for all the distributions of the energy landscape which have a random walk statistics, i.e. tend to a Brownian motion distribution in the continuum. These laws can be derived directly by use of the RSRG formalism developed in [11]. They appear there as the large Γ fixed point of RSRG equations describing the flow with Γ of similar renormalized probability distributions. Here, we have made explicit the whole Γ dependence of these probabilities in the special case of an energy landscape made of discrete ± 1 increments.

The nice feature of the formulas (3.24) and (3.27) is that they are precisely those derived in [3] for the limiting probability distribution of the dynamical process itself in its large time scaling regime. In this case, the natural scaling variable is $l \equiv \sigma^2 x / \ln^2(t)$, where $\sigma = 2/T$ is directly related to the expectation value of $\ln^2(p_x/1-p_x)$. We thus recover here the asymptotic equivalence between the statistics of minima and the dynamical process, with the precise correspondence $\Gamma = \ln(t)/\sigma$. Such a relation, valid in principle only for large times, will be tested in Section 4 at shorter times.

Finally, let us mention that a similar computation of the generating function at finite Γ can be performed for landscapes without wall at the origin. The treatment of the degeneracies is however more involved in this case with even more different possible prescriptions. Still, the limiting distribution at large Γ is independent of the chosen prescription. One can also introduce a drift in the problem when drawing the random landscapes. For instance, choosing in (2.1) $\Delta E(x) = 1$ with probability p and $\Delta E(x) = -1$ with probability $q = 1 - p$, we get for, say, $\mathcal{P}_\Gamma^{(1)}$ the expression

$$\mathcal{P}_\Gamma^{(1)}(z) = \frac{1 - 2\, q\, D_\Gamma\left(\sqrt{4pq}\right)}{1 - 2\, q\, z\, D_\Gamma\left(\sqrt{4pqz}\right)} \tag{3.28}$$

Different regimes are obtained according to sign of $p - q$, and to whether $p - q$ is of order one (strong bias) or of order $1/\Gamma$ (weak bias).

To end this section, let us evaluate the first correction to $\mathcal{P}_\infty(s)$ by further expanding the formulas for $\mathcal{P}_\Gamma^{(i)}$ in powers of $1/\Gamma$. We get

$$\mathcal{P}_\Gamma^{(i)}\left(z = 1 - \frac{s}{\Gamma^2}\right) = \left(1 - \frac{a^{(i)}}{\Gamma}\right)\frac{\tanh(\sqrt{2s})}{\sqrt{2s}} + \frac{a^{(i)}}{\Gamma}\left(1 - \frac{3}{2a^{(i)}}\tanh^2(\sqrt{2s})\right) + \mathcal{O}\left(\frac{1}{\Gamma^2}\right)$$
(3.29)

with $a^{(1)} = 2$, $a^{(2)} = 1$ and $a^{(3)} = 3/2$. The above $1/\Gamma$ corrections are probably not universal, i.e. they depend on our particular choice for the statistics of landscapes. Still, the $1/\Gamma$ correction to the *relative* differences $(\mathcal{P}_\Gamma^{(2)} - \mathcal{P}_\Gamma^{(1)})/\mathcal{P}_\Gamma^{(1)}$ and $(\mathcal{P}_\Gamma^{(3)} - \mathcal{P}_\Gamma^{(1)})/\mathcal{P}_\Gamma^{(1)}$ should be universal. Indeed, they involve the proportionality factors between the different $\mathcal{P}_\Gamma^{(i)}$'s, i.e. the factor $D_\Gamma(z)/D_\Gamma(1)$ in (3.18), or the factor $D_\Gamma(z)/(D_\Gamma(z) - D_\Gamma(1))\ln(D_\Gamma(z)/D_\Gamma(1))$ in (3.20). As we already mentioned, $D_\Gamma(z)/D_\Gamma(1)$ is the generating function for the probability $e_\Gamma(x)$ to have the furthest minimum at a distance x from the closest. The proportionality factors above thus concern the *relative* distance between the different degenerate minima, and ignore their absolute position. They are the important statistical quantities to be used when one is interested in the localization property of the dynamical process. If we insist to impose the scaling (3.22) appropriate to absolute positions, we get, for $z = 1 - s/\Gamma^2$

$$\frac{D_\Gamma(z)}{D_\Gamma(1)} = 1 + \frac{1}{\Gamma}\left(1 - \sqrt{2s}\coth(\sqrt{2s})\right) + \mathcal{O}\left(\frac{1}{\Gamma^2}\right)$$

$$\frac{D_\Gamma(z)}{D_\Gamma(z) - D_\Gamma(1)}\ln\left(\frac{D_\Gamma(z)}{D_\Gamma(1)}\right) = 1 + \frac{1}{\Gamma}\left(\frac{1 - \sqrt{2s}\coth(\sqrt{2s})}{2}\right) + \mathcal{O}\left(\frac{1}{\Gamma^2}\right)$$
(3.30)

At large Γ, the factors (3.30) above tend to one. This does not mean that degenerate minima disappear in this limit. Indeed, one can easily compute the probability for having exactly $k + 1$ degenerate minima, equal to:

$$\left(1 - \frac{D_{\Gamma-1}(1)}{2}\right)\left(\frac{D_{\Gamma-1}(1)}{2}\right)^k = \frac{\Gamma + 2}{2(\Gamma + 1)}\left(\frac{\Gamma}{2(\Gamma + 1)}\right)^k$$
(3.31)

Degeneracies do thus exist even at large Γ where the above expression tends to $(1/2)^{k+1}$. However, most of these degeneracies occur at short distances, and not at distances of order Γ^2. Relative distances of order Γ^2 are found only with a probability of order $1/\Gamma$. The $1/\Gamma$ corrections above correspond to situations with exactly *two* degenerate minima at a distance of order Γ^2, as corroborated by the fact that averaging over minima gives half the value obtained by keeping the furthest minimum. Situations with three or more degenerate minima would contribute to higher orders in $1/\Gamma$. At large Γ, the scaling (3.22) is therefore not appropriate to deal with the relative position of degenerate minima. As noticed in (3.14), a non trivial large Γ exists for $D_\Gamma(z)/D_\Gamma(1)$ *without* rescaling of z, involving the Catalan generating function. Expanding (3.14) in z, we obtain

$$e_\Gamma(x) \overset{\Gamma \to \infty}{\to} e(x) \equiv \begin{cases} 0 & \text{if } x \text{ odd} \\ \frac{x!}{2^{x+1}\left(\frac{x}{2}\right)!\left(\frac{x}{2}+1\right)!} & \text{if } x \text{ even} \end{cases}$$
(3.32)

10

If we admit that relative distances between degenerate minima are the appropriate statistical quantities to describe the distance between two diffusing particles, this result without scaling of x at large times agrees with the idea of localization [6]. Still, as explained in [10], the distribution $e(x)$ behaves like $e(x) \sim x^{-3/2}$ at large x. Therefore, its moments $\langle x^\alpha \rangle$ diverge for $\alpha > 1/2$. This divergence comes precisely from the rare configurations (occurring with probability $1/\Gamma$) with two minima at a distance of order Γ^2. They contribute to $\langle x^\alpha \rangle$ by a term $(\Gamma^2)^\alpha / \Gamma = \Gamma^{2\alpha-1}$ which diverges at large Γ for $\alpha > 1/2$ (see [10]).

3.3. Average position of the minimum

From the formulas for the generating functions $\mathcal{P}_\Gamma^{(i)}(z)$, it is straightforward to get the average position $\overline{x}^{(i)}(\Gamma)$ and average squared position $\overline{x^2}^{(i)}(\Gamma)$ of the minimum for the three prescriptions:

$$\overline{x}^{(i)}(\Gamma) = \sum_{x=0}^\infty x p_\Gamma^{(i)}(x) = z \left. \frac{d}{dz} \right|_{z=1} \mathcal{P}_\Gamma^{(i)}(z)$$

$$\overline{x^2}^{(i)}(\Gamma) = \sum_{x=0}^\infty x^2 p_\Gamma^{(i)}(x) = \left(z \frac{d}{dz} \right)^2 \Bigg|_{z=1} \mathcal{P}_\Gamma^{(i)}(z)$$

(3.33)

Expanding (3.21) in powers of $z-1$ around $z=1$ (or in powers of t around $t=0$), we get

$$\overline{x}^{(1)}(\Gamma) = \frac{2\Gamma^2 + 5\Gamma + 3}{3}$$

$$\overline{x}^{(2)}(\Gamma) = \frac{2\Gamma^2 + 7\Gamma + 3}{3}$$

$$\overline{x}^{(3)}(\Gamma) = \frac{2\Gamma^2 + 6\Gamma + 3}{3}$$

(3.34)

and

$$\overline{x^2}^{(1)}(\Gamma) = \frac{16\Gamma^4 + 88\Gamma^3 + 174\Gamma^2 + 147\Gamma + 45}{15}$$

$$\overline{x^2}^{(2)}(\Gamma) = \frac{16\Gamma^4 + 104\Gamma^3 + 226\Gamma^2 + 179\Gamma + 45}{15}$$

$$\overline{x^2}^{(3)}(\Gamma) = \frac{16\Gamma^4 + 96\Gamma^3 + \frac{1780}{9}\Gamma^2 + 163\Gamma + 45}{15}$$

(3.35)

All of them lead to the same large Γ asymptotic formulas

$$\overline{x}^{(i)}(\Gamma) \overset{\Gamma \to \infty}{\sim} \frac{2}{3}\Gamma^2$$

$$\overline{x^2}^{(i)}(\Gamma) \overset{\Gamma \to \infty}{\sim} \frac{16}{15}\Gamma^4$$

(3.36)

This asymptotic behavior involves only the scaling variable x/Γ^2 and the exact prefactors can be directly obtained from the limiting distribution (3.24) by a suitable expansion in s around $s=0$. We have in particular the asymptotic relation

$$\overline{x^2} \sim \frac{12}{5}(\overline{x})^2$$

(3.37)

11

Here again, the difference for the subleading terms in (3.34) and (3.35) for the three prescriptions comes from landscapes with two degeneracies separated by a distance of order Γ^2. Such configurations, occuring with probability $\sim 1/\Gamma$, yield a correction of order $\Gamma^2/\Gamma = \Gamma$ to $\overline{x}(\Gamma)$ and a correction of order $\Gamma^4/\Gamma = \Gamma^3$ to $\overline{x^2}(\Gamma)$. For these situations with exactly *two* effective degenerate minima, it is equivalent to take the average over the minima (prescription (3)) and to average over the closest and the furthest minimum (prescriptions (1) and (2)). This explains why the subleading coefficient in the prescription (3) is exactly the average of the subleading coefficients of prescriptions (1) and (2). Situations with three degenerate minima distant from $\sim \Gamma^2$ occur with probability $\sim 1/\Gamma^2$ and influence the sub-subleading coefficient. Note also that the constant term in (3.34) and (3.35) must be the same for the three prescriptions since, for $\Gamma = 0$, there cannot be any degeneracy of the deepest minimum. The above arguments explain why $\overline{x}^{(3)}(\Gamma)$ is exactly the average of $\overline{x}^{(1)}(\Gamma)$ and $\overline{x}^{(2)}(\Gamma)$ and why $\overline{x^2}^{(3)}(\Gamma)$ differs form the average of $\overline{x^2}^{(1)}(\Gamma)$ and $\overline{x^2}^{(2)}(\Gamma)$ by a term of order Γ^2 only.

In order to have a precise measure of the subleading terms, we introduce the quantity

$$\chi_\Gamma^{(i)} = \frac{\overline{x^2}^{(i)}(\Gamma)}{\left(\frac{12}{5}\right)\left(\overline{x}^{(i)}(\Gamma)\right)^2} - 1 \tag{3.38}$$

with a factor 12/5 chosen to eliminate the leading large Γ term, so that $\chi_\Gamma^{(i)} \sim 1/\Gamma$ tends to zero at large Γ. Remarkably, in the case (3), an extra cancelation occurs, leading to $\chi_\Gamma^{(3)} \sim 1/\Gamma^2$. In the following section, we compare this quantity, as computed from (3.34) and (3.35), with a similar quantity defined for the dynamical model.

4. Dynamics

4.1. Simulation

Beside the above theoretical statistical predictions, we have made a numerical study of the dynamics (2.2) of a particle for a large sample of quenched random potentials drawn to satisfy the relations (2.1).

For each drawn landscape, we calculate the probability $P(x,t)$ that the particle sits at position x at time t. Due to the discrete nature of the landscape, it is possible to make an *exact* enumeration of all the possible walks arriving at a given position x at some time t, and to evaluate their probability deduced from (2.2) for the particular chosen landscape.

A more efficient way to implement this enumeration is to calculate $P(x,t)$ exactly step by step in time from the master equation

$$P(x, t+1) = p_{x-1}P(x-1, t) + q_{x+1}P(x+1, t) \tag{4.1}$$

with p_x and $q_x = 1 - p_x$ the probabilities of jumping from site x respectively to the right and to the left, as explicited in (2.2), with in particular $p_0 = 1 - q_0 = 1$ and with the convention $p_{-1} = 0$. The master equation is supplemented by the initial condition $P(x, 0) = \delta_{x,0}$. The

computed probability $P(x,t)$ is then averaged over all the energy landscapes of our sample (the sample size is 10^5 energy landscapes for most simulations).

At any finite t, it is clear that the particle cannot reach a position $x > t$, hence $P(x,t) = 0$ exactly for all $x > t$. The normalization of the probability requires that $\sum_x P(x,t) = 1$ at any time t. In practice, the probability to occupy sites far from the origin is extremely low. To reduce the computation time, we drop the normalization condition and replace it by

$$\sum_x P(x,t) > 1 - \varepsilon \tag{4.2}$$

where $\varepsilon \ll 1$. Therefore, instead of describing the complete accessible landscape of size $x = t$ at time t, we fix the maximal size at a much smaller value of x such that the condition (4.2) is fulfilled for all our energy landscapes. Of course, the choice of this size depends crucially on the temperature T and on the number of iterations. In practice, we take $\varepsilon = 0.01$ for most simulations and we checked that this simplification does not lead to significant errors. The computation time is significantly reduced for low temperatures, since the effectively visited landscape is of much smaller size. With this simplification, we were able to study the dynamics up to 10^5 iterations for low temperature regimes (10^4 for $T = 2$).

Note that for our particular choice of dynamics, the particle cannot stay at the same site for two consecutive times t and $t + 1$. Thus $P(2x + 1, 2t) = P(2x, 2t + 1) = 0$. As we already mentioned, the net effect of this parity condition is to create residual fluctuations, which persist even at $T = 0$, where barriers of height $\Gamma = 1$ can always be passed. This will explain in particular why, at $T = 0$, some equilibration can take place between all the deepest minima accessible by passing $\Gamma = 1$-barriers. In the following subsections, we always present results for times of a well defined (even) parity.

It is instructive to visualize the typical evolution of $P(x,t)$ with time for a fixed landscape before making the quenched average over our sample of landscapes. Figure 4 shows such an evolution with 10^7 iterations. One clearly sees that the regions with a large probability of occupation are concentrated around local minima of the potential. As t increases, these high density regions migrate to deeper minima. The duration of occupation of a local minimum in logarithmic scale is roughly proportional to the height of the energy barrier on its right.

4.2. Distribution P(x,t)

Let us first present our numerical results for the distribution $P(x,t)$. We will use overbars to denote the average over our sample of landscapes, while brackets $\langle \cdot \rangle$ will denote the thermal average estimated from the probability $P(x,t)$ computed for a fixed landscape. We are interested here in the average distribution $\overline{P(x,t)}$ at a *fixed* large enough time. From the asymptotic large Γ results (3.26) and (3.36), we expect that, at large t,

$$\overline{\langle x \rangle}(t)\overline{P(x,t)} \sim \frac{2}{3} \, p_\infty \left(\frac{2}{3} \frac{x}{\overline{\langle x \rangle}(t)} \right) \tag{4.3}$$

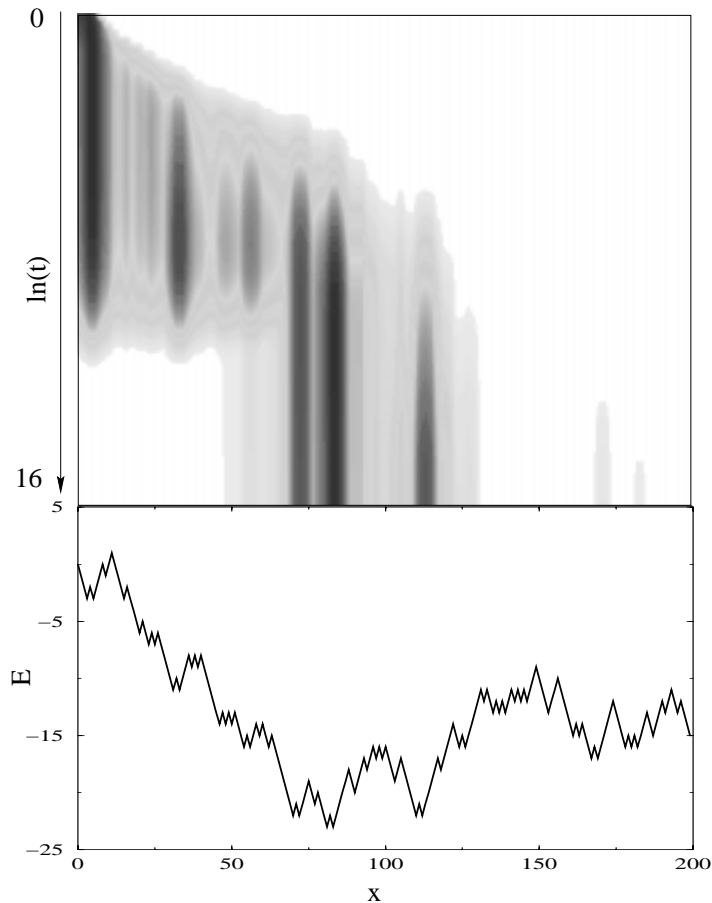with p_∞ given by (3.27).

Fig.4: Evolution with time (in logarithmic scale) of the distribution $P(x,t)$ in a given energy landscape (drawn below). The evolution runs over 10^7 iterations. The intensity in the greyscale is proportional to $-\ln P(x,t)$, i.e. darker regions correspond to higher values of $P(x,t)$.

Figure 5 shows our results for $T = 1/2$ and different values of t. The agreement with the asymptotic exact formula is apparently very good. To have a better quantitative evaluation of how close we are to the asymptotic result, we will study in the next section the first and second moments of the distribution. As we shall see, significant deviations do actually exist, some of which can be well explained by our finite Γ corrections to the asymptotic statistics. We will also discover some interesting underlying oscillatory behaviors.

4.3. Results for the first and second moments and comparison with the statistics of minima

We present here our numerical results for the average position $\overline{\langle x \rangle}(t)$ and average squared position $\overline{\langle x^2 \rangle}(t)$ for varying time t and at various temperatures. We first check if $\overline{\langle x^2 \rangle}(t)$ and $(\overline{\langle x \rangle}(t))^2$ obey the expected asymptotic relation (3.37) with a proportionality factor $12/5$. Note that for a purely diffusive system in a homogeneous medium (i.e. in a flat energy landscape) where $\langle x \rangle(t) \sim \sqrt{t}$, a similar relation holds, but with a smaller proportionality factor $\pi/2$.
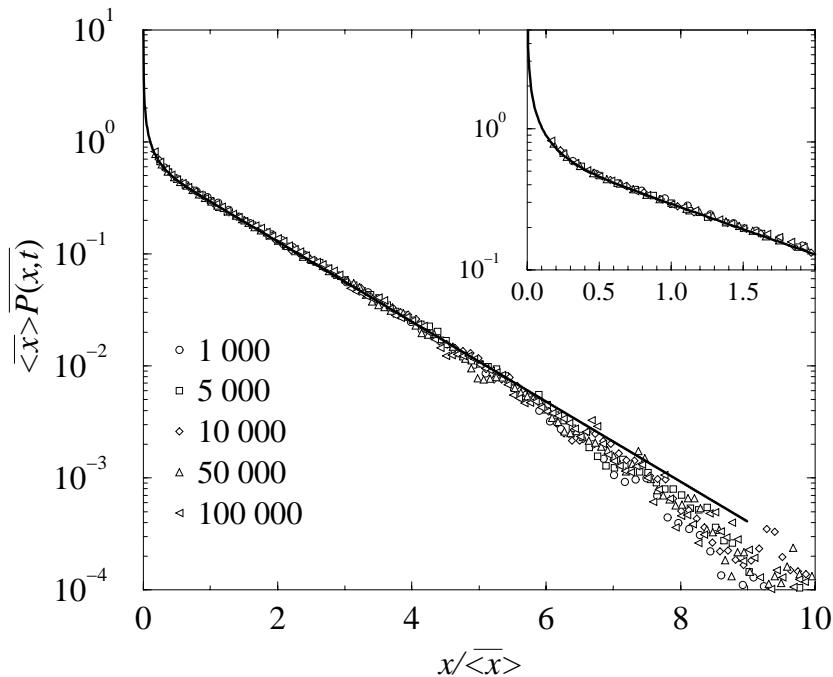
14

Fig.5: The rescaled average distribution $\overline{\langle x \rangle}(t)\overline{P(x,t)}$ as a function of the rescaled variable $x/\overline{\langle x \rangle}(t)$ at $T = 1/2$ and for various values of the time $t = 1\,000, 5\,000, 10\,000, 50\,000$ and $100\,000$. The solid line indicates the exact asymptotic formula as given by (4.3) and (3.27).

Figure 6 presents the corresponding data for several temperatures from $T = 2/5$ to $T = 2$. For the range of $\overline{\langle x \rangle}^2$ presented here, the asymptotic formula (3.37) and the more complete statistical relations obtained from our finite Γ predictions by eliminating Γ between (3.34) and (3.35) do not differ significantly. We therefore expect, if the dynamics follows the statistics of minima, that the asymptotic linear relation is verified in the whole range of $\overline{\langle x \rangle}^2$. This is precisely what we observe at low temperatures (below $T \sim 1$). In this regime, a more refined analysis will reveal very interesting underlying oscillatory behaviors, as emphasized below. At high temperatures (above $T \sim 1$), we see a significant deviation from the expected law, with a behavior closer to a purely diffusive regime at small $\overline{\langle x \rangle}^2$. Still, even at $T = 2$ (see inset in Figure 6), the correct slope is eventually recovered at large $\overline{\langle x \rangle}^2$. In this range of temperatures, the observed deviation is not explained by our finite Γ corrections to the asymptotic law p_∞, but is more simply the effect of a short time diffusion regime in which the particle does not yet feel the random potential. Such a regime will last until the particle reaches a distance x such that $E(x) \sim \sqrt{x} \sim T$, i.e up to a transition time $t \sim x^2 \sim T^4$.

For a comparison of our data with the statistics of minima of the previous section, we need to consider instead of the first and second moments more refined quantities which in
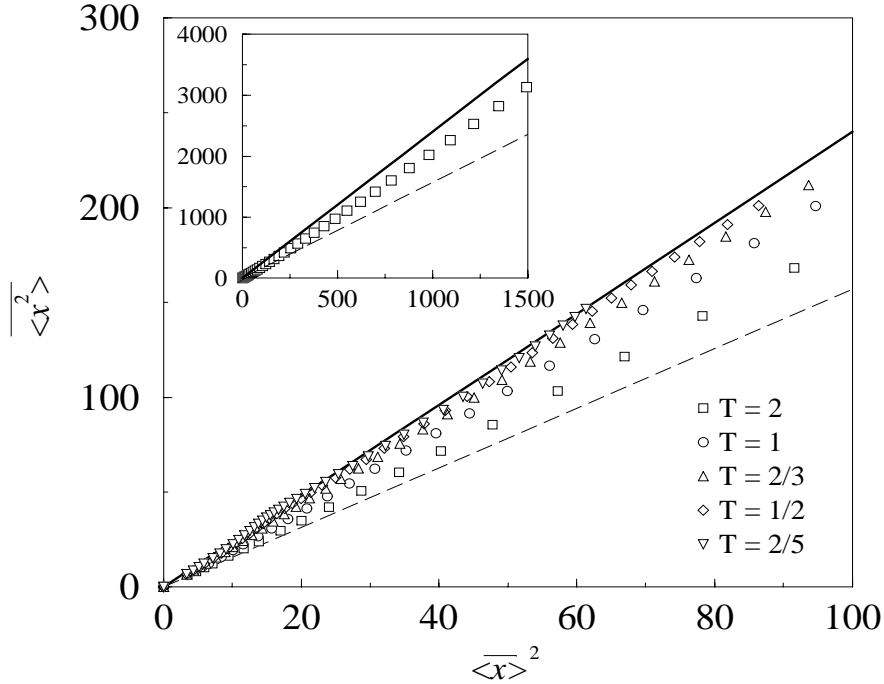
Fig.6: A numerical check of the relation (3.37). The solid line has the slope 12/5 expected from (3.37) while the dashed line has the slope $\pi/2$ expected for the normal diffusion is a flat landscape. For $T = 2$, a broader window of $\overline{\langle x \rangle}^2$ (see inset) is needed to recover the asymptotic law.

practice contain exactly the same information but are more adequate for our purposes since they clearly emphasize the finite Γ corrections. Anticipating our conclusions, we focus on the statistics (3) which corresponds to an averaging over degenerate minima. Inverting the formula (3.34) for the prescription (3), we consider instead of $\overline{\langle x \rangle}(t)$ the equivalent quantity:

$$\Gamma(t) \equiv \frac{-3 + \sqrt{3 + 6\overline{\langle x \rangle}(t)}}{2} \tag{4.4}$$

such that $\overline{x}^{(3)}(\Gamma(t)) = \overline{\langle x \rangle}(t)$. The quantity $\Gamma(t)$ is thus an estimate of the effective height of the barriers which can be passed at the time scale t, obtained by matching the first moment measured in the dynamical process with the average position of the minima resulting from the formula (3.34) in case (3).

Figure 7 shows $\Gamma(t)$ as a function of $\ln(t)$ for different values of the temperature. At low temperature, $\Gamma(t)$ oscillates around an average straight line and develops plateaus at *integer* values of Γ. These plateaus are of course a signature of the underlying discrete nature of the landscape, and are an indication of the actual relation between the dynamics and a process of passing increasing discrete barriers. This effect disappears at higher temperatures. Discarding these oscillations, the curves have an average linear growth with a slope directly proportional to the temperature. More precisely, we can reasonably fit
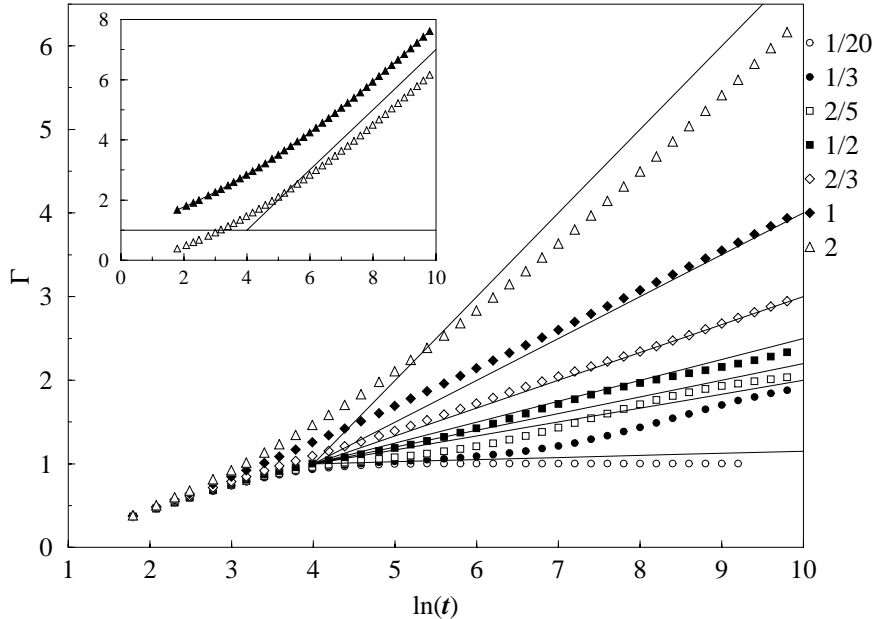
16

Fig.7: The quantity $\Gamma(t)$ as defined by Eq. (4.4) for $T = 1/20$ to $T = 2$, as a function of $\ln(t)$. The solid lines show the corresponding fits of Eq. (4.4) for the average linear growth of the curves remaining after discarding the superimposed oscillations. The use of the complete formula (4.4) is necessary to obtain the correct position of the fit at low temperatures. At high temperature ($T = 2$ in the inset), the fit (4.4) is better if we define $\Gamma(t)$ by the asymptotic formula $\Gamma(t) \sim \sqrt{(3/2)\overline{\langle x \rangle}(t)}$

this average linear growth by the formula (see Figure 7: for the oscillating curves, the fits reasonably match the maxima of the oscillations)

$$\Gamma(t) = \frac{T}{2}\ln\left(\frac{t}{t_0}\right) + 1 \tag{4.5}$$

with $\ln(t_0) \sim 4$. The proportionality factor $1/2 = T/\sigma$ between $\Gamma(t)$ and $T\ln(t)$ is that expected from the correspondence between statistics and dynamics in the asymptotic limit, as already discussed. At low temperature and shorter times, this correspondence is still reasonably good, apart from the superimposed oscillations. The additive constant 1 in (4.5) can be understood as the effect of the "residual fluctuations" which remain at $T = 0$ from the parity condition and make the barriers of height $\Gamma = 1$ always passable. To obtain the correct position of the linear fit, we definitely had to use the complete formula (4.4), which presents a shift of $-3/2$ with respect to the asymptotic relation $\Gamma(t) \sim \sqrt{(3/2)\overline{\langle x \rangle}(t)}$ obtained from (3.36). This reflects the importance of the finite Γ corrections at low temperatures. For higher temperature however ($T = 2$), we obtain a better scaling with the asymptotic law without shift (see the inset in Figure 7, black triangles) than with the shift

(white triangles). Again at high temperatures, the deviation from the asymptotic limit is not explained by finite Γ corrections alone.

We now analyze our data for the second moment $\overline{\langle x^2 \rangle}(t)$. Here again, we prefer to consider the more adequate quantity

$$\chi(t) = \frac{\overline{\langle x^2 \rangle}(t)}{\left(\frac{12}{5}\right)\left(\overline{\langle x \rangle}(t)\right)^2} - 1 \qquad (4.6)$$

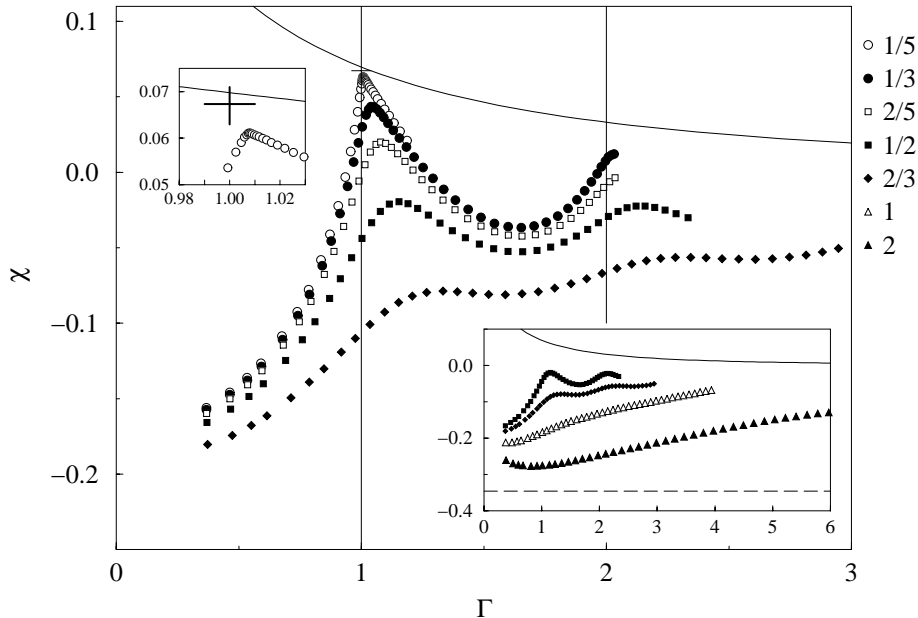copied from (3.38) to measure the deviation from the asymptotic regime (3.37).

Fig.8: The quantity $\chi(t)$ defined by Eq. (4.6) as a function of $\Gamma(t)$ for temperatures ranging from $T = 1/5$ to $T = 2$. The solid line shows the statistical estimate $\chi_\Gamma^{(3)}(\Gamma)$ as defined by Eq. (3.38). The cross in the inset indicates the small corrections at $\Gamma = 1$ to this statistical value due to parity effects, as computed in Appendix A. The dashed line in the lower inset indicates the value of χ for pure diffusion in flat landscape.

Figure 8 presents our results for $\chi(t)$ versus $\Gamma(t)$, and a comparison with the corresponding statistical relation calculated from the previous section between $\chi_\Gamma^{(3)}$ and Γ. We recover again a low temperature regime with oscillations and a high temperature regime without oscillations. In this high temperature regime, the asymptotic limit is reached very slowly and the short time dependence is different from the finite Γ predictions for the statistics of minima. The subleading short time corrections to the universal asymptotic behavior are thus different from that predicted by the statistics of minima. At low temperature however, the oscillations of χ are peaked around integer values of Γ, and sharpen

18

as the temperature decreases to zero. In this limit $T \to 0$, the height of the peaks tend precisely to the value of $\chi_\Gamma^{(3)}$ at the corresponding integer. We thus recover our predictions for the statistics of minima, which strictly speaking are valid only for integer values of the barrier Γ. We also observe two additional dynamical effects:

- Between two consecutive integer values $\Gamma - 1$ and Γ, we find a transition regime with a strong depletion of χ. We interpret this effect as resulting from a period of equilibration of the particle passing from the statistics of minima at scale $\Gamma - 1$ to that at scale Γ.
- As the temperature increases, the peaks are rounded and their maxima slowly move to lower values of χ. The peaks eventually disappear at high temperature.

We interpret the above results as follows. From the formula (4.5), the barriers of height Γ are passed at times of order $t(\Gamma) \sim t_0 \exp[2(\Gamma - 1)/T]$. After passing these barriers, we admit that the time needed for equilibration in the (always present) degenerate minima is itself of the order of a multiple of $t(\Gamma)$. As the temperature is lowered, the corresponding proportionality factor remains finite due to the residual fluctuations. During the equilibration process at a given Γ, the data get closer to the equilibrium distribution of the minima. The time needed to pass the next barriers, i.e. those of height $\Gamma + 1$ is from (4.5) $t(\Gamma + 1) = t(\Gamma) \exp(2/T)$, that is again a finite multiple of $t(\Gamma)$, depending only on the temperature. In the low temperature regime, the particle thus has enough time to equilibrate and recover the statistics of minima for a fixed passable height Γ *before* it starts passing the barriers of height $\Gamma + 1$. Conversely, at high temperature, the particle keeps finding better and better minima by passing increasing barriers without equilibration for each passed Γ. In particular, the particle does not feel the discrete nature of the potential. This results in the suppression of the oscillations and a behavior closer to normal diffusion.

In the above analysis, the use of statistics (3) is crucial on the one hand to get peaks precisely at integer values of $\Gamma(t)$ and on the other hand to recover the theoretical value of $\chi(\Gamma)$ at the peak for low temperatures. These conditions eliminate the two other statistics. At this level of precision, the purely asymptotic result $\chi = 0$ is also ruled out. As discussed in the Appendix A, the statistics (3) itself must be modified by very small corrections due to parity effects, i.e. the fact that the particle at time t cannot sit right at the correct minima if those happen to have a parity different from t. This effect is sensible only for the peak at $\Gamma = 1$. The corresponding correction is calculated in the Appendix A and leads to a very small reduction ($\sim 3.5\%$) of the peak (see Figure 8), consistent with the data of the dynamical process. The parity correction is more important for quantities which measure the localization of the particle, as we discuss in the next section. The use of a different dynamics allowing the particle to remain at the same site should suppress this correction.

4.4. Localization

In order to have an idea of how localized is the particle, we have measured the probability second moment:

$$Y_2(t) = \overline{\sum_x \left(P(x,t) \right)^2} \tag{4.7}$$

which estimates the probability that two independent particles evolving in the same quenched potential arrive *exactly* at the same site at time t. This quantity is similar

to the participation ratio for localized quantum particles [13]. A non zero value of Y_2 is the signal of a localization. We must however distinguish between two different effects which run counter to this localization and therefore lower Y_2: the effect of temperature which broadens the distribution of a particle around its average position in a minimum, and the existence of several degenerate minima in which the particles can fall. It is this last effect that we measure at very low temperatures. If we assume that, when $T \to 0$, the particle is localized exactly in the deepest minima at scale $\Gamma(t)$, we estimate $Y_2(t)$ by

$$
\begin{aligned}
Y_2(\Gamma) &= \sum_{k=0}^{\infty} \frac{1}{k+1} \frac{\Gamma+2}{2(\Gamma+1)} \left(\frac{\Gamma}{2(\Gamma+1)} \right)^k \\
&= \frac{\Gamma+2}{\Gamma} \ln \left(\frac{2(\Gamma+1)}{\Gamma+2} \right)
\end{aligned}
\tag{4.8}
$$

with $\Gamma = \Gamma(t)$. In the formula above, we used the probability (3.31) to have exactly $k+1$ degenerate minima, weighed by the probability $1/(k+1)$ to have the two particles in the same minimum. In practice, as we already noticed, the formula (4.8) must be corrected to account for the parity effects of the dynamics. At large Γ, this simply amounts to reduce Y_2 by a factor $(\Gamma+2)/(2\Gamma+3) + (1/2) \times (\Gamma+1)/(2\Gamma+3)$ since Y_2 must typically be divided by 2 if the minima have the wrong parity (which occurs with probability $(\Gamma+1)/(2\Gamma+3)$ for even times, see Appendix B) and the particle has to sit on the two neighbors of the minimum. With this estimate, $Y_2(t)$ thus tends at large times ($\Gamma(t) \to \infty$) to a finite value $(1/2) \ln 2$. The same formula (4.8) with the above reduction factor gives also a good estimate at small Γ, with for instance a value $Y_2 \sim (12/5) \ln(4/3) \sim 0.69$ at $\Gamma = 1$. In Appendix B, we present a detailed analysis of the exact corrections for the statistical model at $\Gamma = 1$, leading to a value $Y_2 \sim 0.706415$.

Figure 9 shows our numerical results for $Y_2(t)$ as a function of $\Gamma(t)$. At low temperatures, we recover peaks at integer values of Γ. At low temperatures, the value of the peak at $\Gamma = 1$ is in perfect agreement with the estimate of Appendix B and our results are consistent with a localization of the particle in all the degenerate minima. At high temperatures, $Y_2(t)$ decreases with time but still tends to a finite value at large Γ, apparently proportional to $1/T$. We have also measured the more usual Rényi entropy $H_2(t) = -\overline{\ln(\sum_x P^2(x,t))}$ [9]. In contrast with Y_2, which is an average value over the disorder, $\exp[-H_2]$ gives the *typical* value of the probability for two particles to be at the same site at time t. We find that $\exp[-H_2]$ and Y_2 display the same behavior and differ by a roughly constant multiplicative factor.

Another quantity of interest for the measure of the localization of a particle is the dispersion, defined by

$$
\Delta x^2(t) = \overline{\langle x^2 \rangle(t) - (\langle x \rangle(t))^2}
\tag{4.9}
$$

If the particle were localized in a single minimum, the dispersion $\Delta x^2(t)$ would not grow indefinitely with time (or with Γ) but rather would reach a finite limit. The situation is quite different if, as we expect, the particle is localized in several degenerate minima since, as we already mentioned, minima can be separated by a distance of order Γ^2 with a probability $1/\Gamma$. In this case, Δx^2 grows like $(\Gamma^2)^2/\Gamma = \Gamma^3$ and is thus infinite asymptotically.
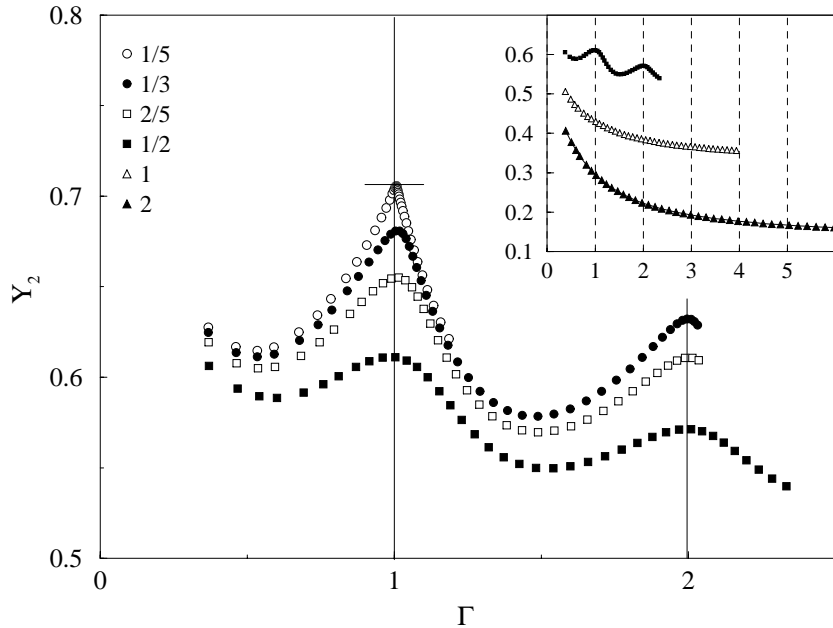
20

Fig.9: The quantity $Y_2(t)$ as defined in Eq. (4.7) as a function of $\Gamma(t)$ for temperatures ranging from $T = 1/5$ to $T = 2$. The horizontal bar is the value of the peak estimated in Appendix B from the statistics with parity corrections.

Figure 10 shows our numerical results for $\Delta x^2(t)$ as a function of $\Gamma(t)$ in logarithmic scales. At low temperatures, the peaks of $\Delta x^2(t)$ follow the statistics (3) of the degenerate minima, with the additional parity corrections, as computed for $\Gamma = 1$ in the appendix B. We thus recover a regime of localization in all the degenerate minima. At high temperatures, $\Delta x^2(t)$ increases rapidly with time, with a scaling compatible with the expected Γ^3 dependence.

5. Conclusions and discussion

We have studied the problem of the one dimensional diffusion of a particle in a semi-infinite quenched random energy landscape with *discrete* integer heights and for different temperatures T. Our data converge to the expected large time universal asymptotic limit, but very slowly (as $1/\ln t$) and the approach to this limit crucially depends on temperature. To quantify the finite time corrections, we have compared our numerical data for the diffusion process at time t with exact results for the statistics of the local minima of the landscapes reached by passing energy barriers of increasing (integer) size Γ. Below $T \sim 1$, we find a low temperature regime in which the dynamical process precisely follows the statistics of minima which corresponds to average over all the degenerate minima at a given scale Γ with the expected correspondence $\Gamma \leftrightarrow T \ln t$. Our data are consistent with a localization of the particle equally distributed in all these degenerate minima. Interesting
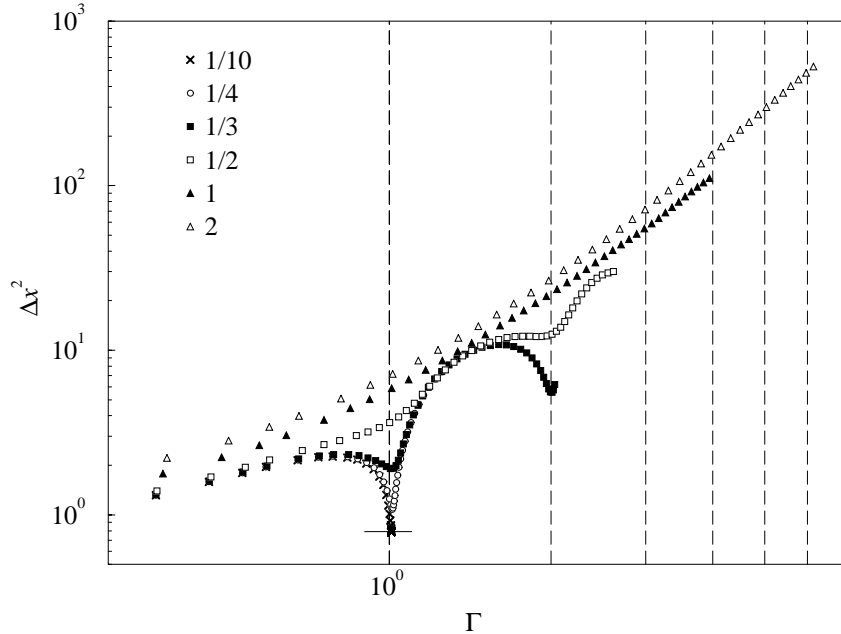
21

Fig.10: The quantity $\Delta x^2(t)$ (in logarithmic scale) as defined in Eq. (4.9) as a function of $\Gamma(t)$ (in logarithmic scale) for temperatures ranging from $T = 1/10$ to $T = 2$. The horizontal bar indicates the value of the peak estimated in Appendix B from the statistics with parity corrections.

transition regimes interpolate between integer values of the scale Γ. At higher temperatures above $T \sim 1$, the approach to the asymptotic laws do not follow the finite Γ corrections to the statistical laws, at least in the regime of times that we consider in our simulation.

We interpret these two different regimes as follows: at small T, the particle has enough time to equilibrate and recovers the statistics at a given Γ before it starts passing barriers of heights $\Gamma + 1$. At high temperatures however, the particle keeps passing barriers of increasing Γ without having enough time for equilibration at a fixed Γ.

A natural question is whether the existence of two regimes is only a finite time effect, or whether it persists for larger times. In the first case, the correspondence between the dynamics and the statistics should be recovered at larger times. In the second case, it is tempting to expect a transition temperature between the two regimes. The low temperature regime would be anyway a consequence of an underlying discrete cut-off for the steps of the energy landscape. The transition temperature would thus be of the order of this cut-off and would tend to zero in the continuum limit where only the high temperature regime would persist.

Acknowledgments

Appendix A. Corrections due to residual fluctuations at $T = 0$

We will concentrate here on our statistics (3), which consists in averaging over all the degenerate minima with equal probability, that is, in the case of k degenerate minima, in assigning a weight factor $1/k$ to each minimum. This statistics implicitly assumes that, after a transition period of equilibration, each degenerate minimum is visited with even probability.

For our particular choice of dynamics however, the particle is not allowed to remain at the same site for two consecutive times t and $t + 1$. As we already mentioned, this results in a parity condition, namely that the particle occupies even sites at even times and odd sites at odd times. Thus, even at $T = 0$, the particle has to fluctuate from odd to even sites. This is what we called "residual fluctuations", which in particular make barriers of height $\Gamma = 1$ always passable, even at $T = 0$, eventually leading to some equilibration between all the deepest minima accessible by passing these $\Gamma = 1$-barriers.

Another effect of these residual fluctuations is that, by preventing the particle to remain seated right in the minima for all times, they create small corrections to the estimates of statistics (3), in particular for the limiting values of the peaks at $T \to 0$ of the quantities χ, Y_2 and Δx^2.

As we will now discuss, these corrections are of two types: a parity correction and a wall correction.

Parity correction: Let us consider a time t with a given parity, say even, so that the particle is forced to occupy sites with the same parity. For a fixed landscape and a fixed Γ, it is clear that all the degenerate deepest minima have a well defined, common parity since returning to the same height requires an even number of steps. This parity however may or may not be that of t. If the two parities coincide, then the particle can fall at $T \to 0$ precisely in the minima and our calculations using statistics (3) are valid. If the two parities do not match, the particle cannot fall right in the deepest minima, but will rather occupy the two neighboring positions on both sides of each minimum. In this case, rather than averaging the positions $x_{\min}^{(m)}$, $m = 1, \ldots, k$ of the k minima with weights $1/k$, we should average the positions $x_{\min}^{(m)} \pm 1$ with weights $1/(2k)$ (of course, if two minima are distant by two elementary steps only, the point in between should receive a weight $1/(2k) + 1/(2k) = 1/k$). What is the probability for the minima to have the wrong parity? Looking at, say, the closest minimum, we can select the even minima by considering the combination $(\mathcal{P}_\Gamma^{(1)}(z) + \mathcal{P}_\Gamma^{(1)}(-z))/2$ and the odd minima by considering $(\mathcal{P}_\Gamma^{(1)}(z) - \mathcal{P}_\Gamma^{(1)}(-z))/2$ instead. The probability for a minimum to be even or odd is thus

$$
\begin{aligned}
\text{Proba(even minima)} &= \frac{1}{2}\left(\mathcal{P}_\Gamma^{(1)}(1) + \mathcal{P}_\Gamma^{(1)}(-1)\right) = \frac{\Gamma + 2}{2\Gamma + 3} \\
\text{Proba(odd minima)} &= \frac{1}{2}\left(\mathcal{P}_\Gamma^{(1)}(1) - \mathcal{P}_\Gamma^{(1)}(-1)\right) = \frac{\Gamma + 1}{2\Gamma + 3}
\end{aligned}
\tag{A.1}
$$

As far as $\overline{x}$ is concerned, it is clear the parity shift creates no correction since $x_{\min}^{(m)}$ is precisely the average of $x_{\min}^{(m)} - 1$ and $x_{\min}^{(m)} + 1$. For $\overline{x^2}$ however, it results in a shift by a

factor:

$$\sum_{m=1}^{k} \frac{1}{2k} \left((x_{\min}^{(m)} - 1)^2 + (x_{\min}^{(m)} + 1)^2 \right) - \frac{1}{k}(x_{\min}^{(m)})^2 = 1 \qquad (\text{A.2})$$

irrespectively of the number of degenerate minima. For even times, we thus get a parity correction to $\overline{x^2}$ equal to $1 \times (\Gamma + 1)/(2\Gamma + 3)$. This correction is negligible at large Γ but can be measured at $\Gamma = 1$, where it predicts a shift of $2/5$ to $\overline{x^2}^{(3)}(1)$. The same effect is more sensible for Y_2 and Δx^2, and will be discussed in the Appendix B.

Wall correction: Another correction comes from the presence of the wall at $x = 0$ in the particular case where $x_{\min} = 0$ itself is a minimum. This situation occurs with probability:

$$\mathcal{P}_\Gamma^{(1)}(0) = \frac{1}{\Gamma + 2} \qquad (\text{A.3})$$

Let us thus assume that $x_{\min}^{(1)} = 0$ is the first deepest minimum, together with $(k-1)$ other minima at even positions $x_{\min}^{(m)}$, $m = 2, \ldots k$. Let us also assume that t is even so that the particle can sit precisely in these minima. Still, after equilibration, the minimum at $x_{\min}^{(1)} = 0$ is less probable that the other minima. This effect is visible at $T = 0$ and $\Gamma = 1$ where the equilibration is due to residual fluctuations only.
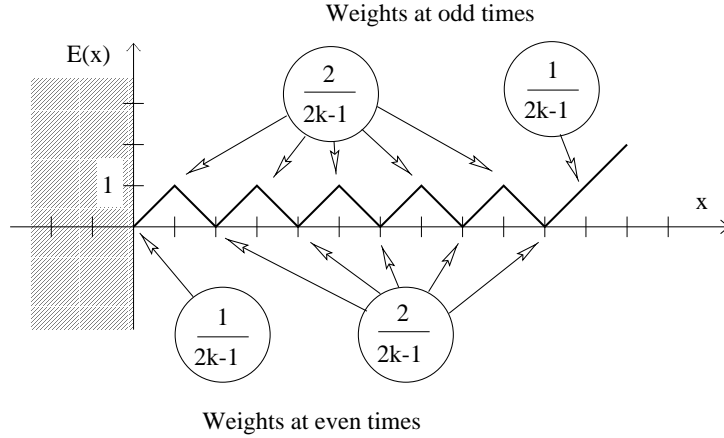

Weights at odd times

Weights at even times

Fig.11: The modified equilibrium weights for k degenerate minima at $\Gamma = 1$ in the case of a first minimum right at the wall. Each weight at even times is the average of the neighboring weights at odd times and conversely.

In this case (see Figure 11), the k minima are at positions $x_{\min}^{(m)} = 2m - 2$. Since the minimum at $x_{\min}^{(1)}$ has no accessible neighbor on its left, it is easy to see that, at even times, this minimum is less probable that the others by a factor of 2, leading to a probability $1/(2k-1)$ for this minimum and a probability $2/(2k-1)$ for the $(k-1)$ others, instead of an equal probability $1/k$ for each minimum. The correction to $\overline{x}^{(3)}(1)$ is thus:

$$\left(\frac{2}{2k-1} - \frac{1}{k} \right) \sum_{m=2}^{k} (2m - 2) = \frac{k-1}{2k-1} \qquad (\text{A.4})$$

and that to $\overline{x^2}^{(3)}(1)$:

$$\left(\frac{2}{2k-1} - \frac{1}{k}\right) \sum_{m=2}^{k} (2m-2)^2 = \frac{2}{3}(k-1) \qquad (\text{A.5})$$

According to (3.31) and (A.3), such a situation occurs with probability $(1/3) \times (3/4)(1/4)^{k-1}$

Combining the parity correction and the wall correction, we get

$$\overline{x}_{\text{corr.}} = \overline{x}^{(3)}(1) + \frac{1}{3} \times \sum_{k=1}^{\infty} \frac{3}{4}\left(\frac{1}{4}\right)^{k-1} \frac{k-1}{2k-1} = \frac{92 - 3\ln(3)}{24} \qquad (\text{A.6})$$

instead of $\overline{x}^{(3)}(1) = 11/3$, i.e. numerically 3.696 instead of 3.666, and

$$\overline{x^2}_{\text{corr.}} = \overline{x^2}^{(3)}(1) + \frac{2}{5} \times 1 + \frac{1}{3} \times \sum_{k=1}^{\infty} \frac{3}{4}\left(\frac{1}{4}\right)^{k-1} \frac{2}{3}(k-1) = \frac{4724}{135} \qquad (\text{A.7})$$

instead of $\overline{x^2}^{(3)}(1) = 932/27$, i.e. numerically 34.99 instead of 34.52. With these values, the estimate $\chi_1^{(3)} = 0.06978$ is modified into $\chi_{\text{corr.}} = 0.06733$, i.e. is lowered by 3.5% only.

Appendix B. Computation of Y_2 and Δx^2 in the limit $T \to 0$

In this Appendix, we will calculate the value of the peak at $T \to 0$ and $\Gamma = 1$ of Y_2 and Δx^2. These value are very sensitive to the residual fluctuations. We will thus follow the same lines as in the previous Appendix. We will consider even times and a situation with k degenerate minima at positions $x_{\text{min}}^{(m)} = x_{\text{min}}^{(1)} + 2m - 2$, $m = 1, \ldots, k$. According to (3.31), this situation occurs with probability $(3/4)(1/4)^{k-1}$. We distinguish between three possibilities for the first minimum:

(i) $x_{\text{min}}^{(1)} = 0$. According to (A.3), this occurs with probability $1/3$.

(ii) $x_{\text{min}}^{(1)}$ is odd. According to (A.1),this occurs with probability $2/5$.

(iii) $x_{\text{min}}^{(1)}$ is even and non zero. This occurs with probability $1 - 1/3 - 2/5 = 4/15$.

The weights associated to the minima (or their neighbors) in the three situations are depicted in Figure 12. The corresponding contributions to Y_2 are

$$\left(\frac{1}{2k-1}\right)^2 + (k-1)\left(\frac{2}{2k-1}\right)^2 = \frac{4k-3}{(2k-1)^2} \quad \text{in case (i)}$$

$$\left(\frac{1}{2k}\right)^2 + (k-1)\left(\frac{1}{k}\right)^2 + \left(\frac{1}{2k}\right)^2 = \frac{2k-1}{2k^2} \quad \text{in case (ii)} \qquad (\text{B.1})$$

$$k\left(\frac{1}{k}\right)^2 = \frac{1}{k} \quad \text{in case (iii)}$$
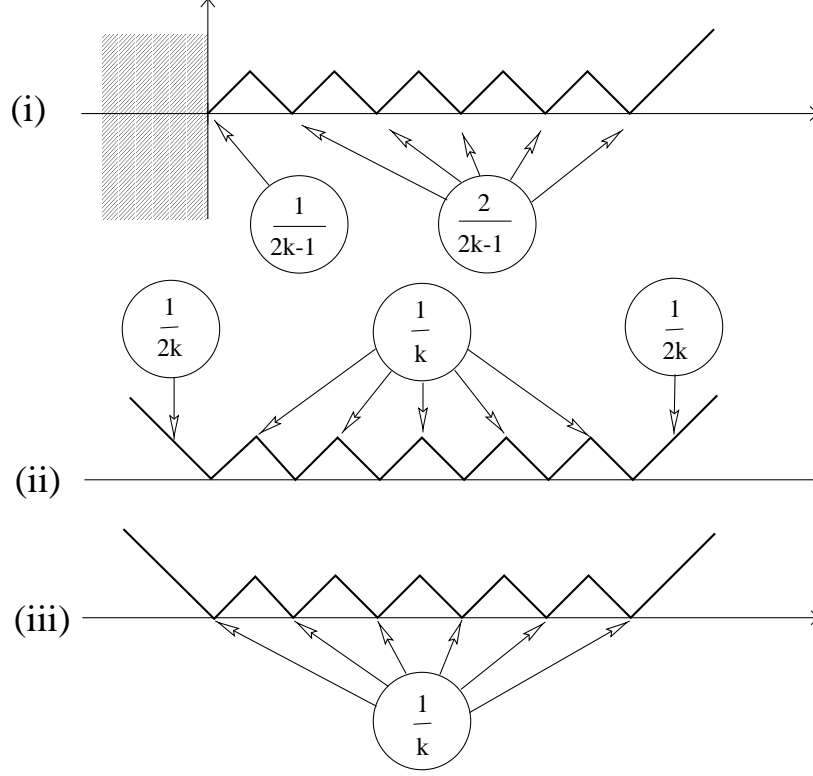
Fig.12: Respective weights of accessible minima at even times for $\Gamma = 1$ in the three situations: (i) the first minimum is right at the wall; (ii) the first minimum is at an odd position; (iii) the first minimum is at an even position but not at the wall.

Combining these contributions with their respective weights, we get

$$Y_2 = \sum_{k=1}^{\infty} \frac{3}{4} \left(\frac{1}{4}\right)^{k-1} \left\{ \frac{1}{3} \times \frac{4k-3}{(2k-1)^2} + \frac{2}{5} \times \frac{2k-1}{2k^2} + \frac{4}{15} \times \frac{1}{k} \right\} \qquad (\text{B.2})$$

$$= 0.706415$$

Similarly, the contributions to Δx^2 are

$$\frac{2}{2k-1} \sum_{m=2}^{k} (2m-2)^2 - \left(\frac{2}{2k-1} \sum_{m=2}^{k} (2m-2) \right)^2 = \frac{4k(k^3 - 2k^2 + 2k - 1)}{3(2k-1)^2} \quad \text{in case (i)}$$

$$(\text{B.3})$$

$$\frac{1}{2k}(x_{\min}^{(1)} - 1)^2 + \frac{1}{k} \sum_{m=2}^{k} (x_{\min}^{(1)} + 2m - 3)^2 + \frac{1}{2k}(x_{\min}^{(1)} + 2k - 1)^2$$

$$- \left(\frac{1}{2k}(x_{\min}^{(1)} - 1) + \frac{1}{k} \sum_{m=2}^{k} (x_{\min}^{(1)} + 2m - 3) + \frac{1}{2k}(x_{\min}^{(1)} + 2k - 1) \right)^2 = \frac{k^2 + 2}{3} \quad \text{in case (ii)}$$

$$(\text{B.4})$$

26

$$\frac{1}{k}\sum_{m=1}^{k}(x_{\min}^{(1)} + 2m - 2)^2 - \left(\frac{1}{k}\sum_{m=1}^{k}(x_{\min}^{(1)} + 2m - 2)\right)^2 = \frac{k^2 - 1}{3} \quad \text{in case (iii)} \qquad (\text{B.5})$$

Combining these contributions with their respective weights, we get

$$\Delta x^2 = \sum_{k=1}^{\infty}\frac{3}{4}\left(\frac{1}{4}\right)^{k-1}\left\{\frac{1}{3}\times\frac{4k(k^3 - 2k^2 + 2k - 1)}{3(2k-1)^2} + \frac{2}{5}\times\frac{k^2 + 2}{3} + \frac{4}{15}\times\frac{k^2 - 1}{3}\right\}$$

$$= 0.789288$$

$$(\text{B.6})$$

References

[1] H. Kesten, M.W. Koslow and F. Spitzer, *Compos. Math.*, **30**, 145-168, (1975)

[2] Ya. G. Sinai, *Theor. Proba. Appl.*, **27**, 256-268, (1982)

[3] A.O. Golosov, *Soviet Math. Dokl.*, **28**, 18-22, (1983)

[4] H. Kesten, *Physica A*, **138**, 299-309, (1986)

[5] A.O. Golosov, *Russ. Math. Surveys*, **41**, 199-201, (1986)

[6] A.O. Golosov, *Commun. Math. Phys.*, **92**, 491-506, (1984)

[7] J.-P. Bouchaud, A. Comtet, A. Georges and P. Le Doussal, *Ann. Phys.*, **201**, 285-341, (1990)

[8] A. Bunde, S. Havlin, H.E. Roman, G. Schildt and H.E. Stanley, *J. Stat. Phys.*, **50**, 1271-1276, (1988)

[9] P. Grassberger and R. Leuverink, *J. Phys. A: Math. Gen.*, **23**, 773-780, (1990)

[10] L. Laloux and P. Le Doussal, *Phys. Rev. E*, **57**, 6296-6326, (1998), (cond-mat/9705249)

[11] D.S. Fisher, P. Le Doussal and C. Monthus, *Phys. Rev. Lett.*, **80**, 3539-3542, (1998), (cond-mat/9710270)

[12] P. Di Francesco, O. Golinelli and E. Guitter, *Commun. Math. Phys.*, **186**, 1-59, (1997), (cond-mat/9602025)

[13] A. Compte and J.-P. Bouchaud, *J. Phys. A.: Math. Gen.*, **31**, 6113-6121, (1998), (cond-mat/9801140)